ACS APPLIED ENERGY MATERIALS

www.acsaem.org

Letter

Operando Transmission Electron Microscopy Study of All-Solid-State Battery Interface: Redistribution of Lithium among Interconnected Particles

Shibabrata Basak,* Vadim Migunov, Amir H. Tavabi, Chandramohan George, Qing Lee, Paolo Rosi, Violetta Arszelewska, Swapna Ganapathy, Ashwin Vijay, Frans Ooms, Roland Schierholz, Hermann Tempel, Hans Kungl, Joachim Mayer, Rafal E. Dunin-Borkowski, Rüdiger-A. Eichel, Marnix Wagemaker, and Erik M. Kelder

Cite This: *ACS Appl. Energy Mater.* 2020, 3, 5101−5106

Read Online

ACCESS | Metrics & More | Article Recommendations | Supporting Information

ABSTRACT: With operando transmission electron microscopy visualizing the solid−solid electrode−electrolyte interface of silicon active particles and lithium oxide solid electrolyte as a model system, we show that (de)lithiation (battery cycling) does not require all particles to be in direct contact with electrolytes across length scales of a few hundred nanometers. A facile lithium redistribution that occurs between interconnected active particles indicates that lithium does not necessarily become isolated in individual particles due to loss of a direct contact. Our results have implications for the design of all-solid-state battery electrodes with improved capacity retention and cyclability.

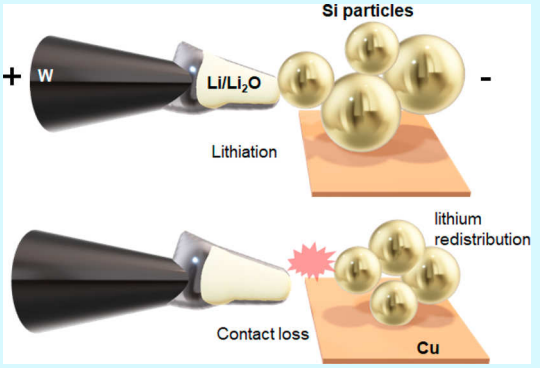

KEYWORDS: *operando TEM, electron microscopy, all-solid-state batteries, electrode−electrolyte interface, (de)lithiation*

Safety features of Li-ion batteries are a high priority requirement as their adoption in electric vehicles and day-to-day electronic devices[1,2] is continuously increasing. The liquid electrolytes that are typically used in traditional Li-ion batteries are flammable, especially at higher operating voltages[3] and temperatures. By contrast, an all-solid-state battery (ASSB) makes use of a solid electrolyte instead of a liquid electrolyte, which reduces the risk of flammability.[4,5] Despite this advantage, the lower ionic conductivity of solid electrolytes[6,7] compared to liquid electrolytes had set the first limitation on the development of ASSBs. However, recent developments in sulfur-containing solid electrolytes, such as $Li_{10}GeP_2S_{12}$, $Li_{9.54}Si_{1.74}P_{1.44}S_{11.7}Cl_{0.3}$, Li_6PS_5X (X = Cl, Br, I), and $Li_7P_3S_{11}$, achieved Li-ion conductivities that are comparable to or greater than those of liquid electrolytes[8−11] and have thrown this research area open. It was further shown that the presence of the solid−solid electrolyte−electrode interface in ASSBs[12] introduces additional problems[13−16] that are very different from those of the traditional liquid−solid electrode−electrolyte interface (Figure 1a,b). First, in batteries containing liquid electrolytes, the entire surface of the electrode particles is wetted by electrolytes, whereas the electrode particles and solid electrolytes in ASSBs are connected primarily at point contacts, which are limited in terms of their numbers (as not all electrode particles are in direct contact with electrolyte particles); therefore, ionic transport is basically restricted,[17] diminishing the specific capacity of these batteries. Decomposition reactions at electrode−electrolyte interfaces during battery cycling causing the formation of passivating layers as well as electrode volume changes during battery cycling result in the loss of contacts between the electrode and electrolyte particles (as in Figure 1b), further decreasing direct ion exchange pathways. Second, inhomogeneous (de)lithiation through point contacts can induce strain, which affects electrode mechanical integrity leading to capacity fade.

Silicon as an alloying-type electrode material is virtually ideal for studying (de)lithiation processes, in particular, volume expansion and strain induced cracking via *in situ* TEM. For example, McDowell et al. have shown that Li can diffuse through small Si particles and flow from nanowires to nanoparticles, which is characterized by anisotropic lithiation and volume expansion of particles. As lithiation of crystalline Si is

Received: March 12, 2020
Accepted: May 8, 2020
Published: May 8, 2020

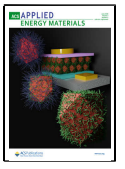

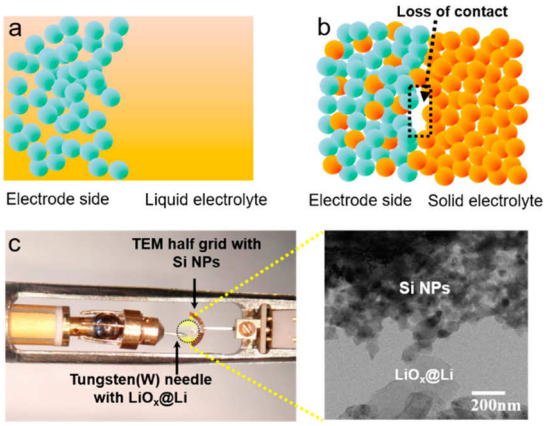

Figure 1. Schematics: (a) The electrode surface is wetted by liquid electrolytes in a traditional Li-ion cell; (b) ion transport in an all-solid-state battery depends on the point contacts, and loss of electrode−electrolyte point contacts during battery cycling can decrease Li-ion exchange pathways. (c) Photograph of part of a Nanofactory TEM specimen holder, onto which a half TEM grid (containing Si nanoparticles) and an electropolished W needle (containing solid electrolyte@Li) were mounted, and a bright-field TEM image showing a micro-ASSB.

predominantly an interface reaction proceeding via a reaction front that is strongly influenced by localized stress, it in turn impacts the extent and rates of lithiation reactions.[18] They have also observed that amorphous Si is involved in two phase lithiation during the first lithiation cycle.[19] Yuk et al. showed that Si lithiation is characterized to be limited by both diffusion and rate of reaction using graphene liquid cell microscopy.[20] Luo et al. reported that Si lithiation is influenced by localized variations in applied voltages affecting the reaction front, which transitioned from being isotropic to anisotropic lithiation, using Si particles and oxidized lithium as the electrolyte.[21] Thus, although there is a significant amount of work on the Si/electrolyte interface, it is mostly focused on lithiation kinetics within the context where active particles are exempted from the problem of losing contact with electrolytes (as uninterrupted electrolyte access is typically achieved in cells with a liquid electrolyte where active particles are soaked as discussed earlier). However, in the case of practical ASSBs (all-solid-state batteries), one of the main problems is active particles losing contact with electrolytes upon battery cycling (Figure 1b). It is therefore imperative to develop an understanding of solid-state battery electrochemistry by taking this loss of electrolyte contact into consideration and studying whether this can potentially deplete cyclable lithium as a result of lithium being trapped in particles upon losing contact with electrolytes, making batteries no longer cyclable. In this Letter, utilizing a Nanofactory TEM[22] specimen holder, we investigate the interface kinetics of ASSB in a nanobattery (Figure 1c) and present evidence for a lithium redistribution process across interconnected active particles when electrode−electrolyte contact is lost.

Operando transmission electron microscopy (TEM) allows for the visualization of (de)lithiation processes in electrode materials at a single particle level in real time.[23,24] Here, we take advantage of the volume change property of Si nanoparticles (NPs) during (de)lithiation[25] to understand the interface kinetics of an ASSB during cycling. The reason why we chose Si as an active particle is because it allows for drastic variation in the number of point contacts with electrolytes, and therefore, the kinetics in terms of Li-ion transport across interfaces in ASSBs can be followed under more realistic conditions where the interparticle connectivity and point contacts are readily impacted by their volume changes. This simulates scenarios similar to real ASSBs which are more prone to suffer from eventual point contact losses over battery cycling. Microbatteries for our operando TEM experiments were assembled by drop-casting Si NPs onto a half TEM grid and by using an

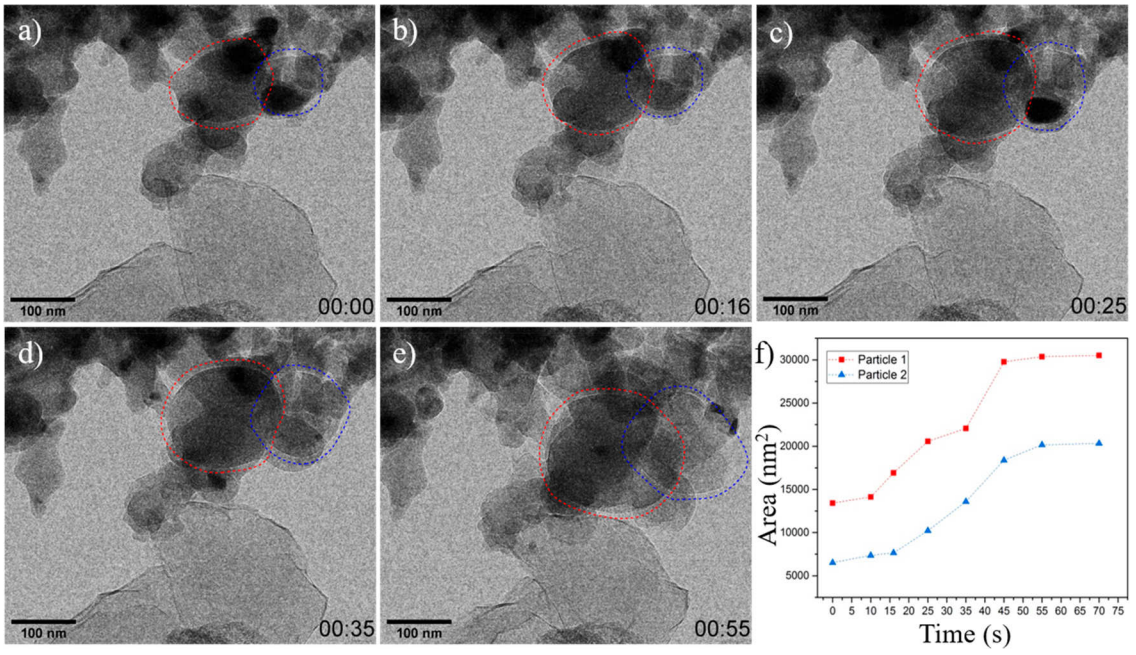

Figure 2. Lithiation of a Si nanoparticle cluster (at a bias of −0.2 V applied). The images were recorded (a) at the start of lithiation and after (b) 16, (c) 25, (d) 35, and (e) 55 s. Two nanoparticles are highlighted in red and blue dotted lines. (f) Changes in the areas of the highlighted nanoparticles plotted as a function of time.

https://dx.doi.org/10.1021/acsaem.0c00543
ACS Appl. Energy Mater. 2020, 3, 5101−5106

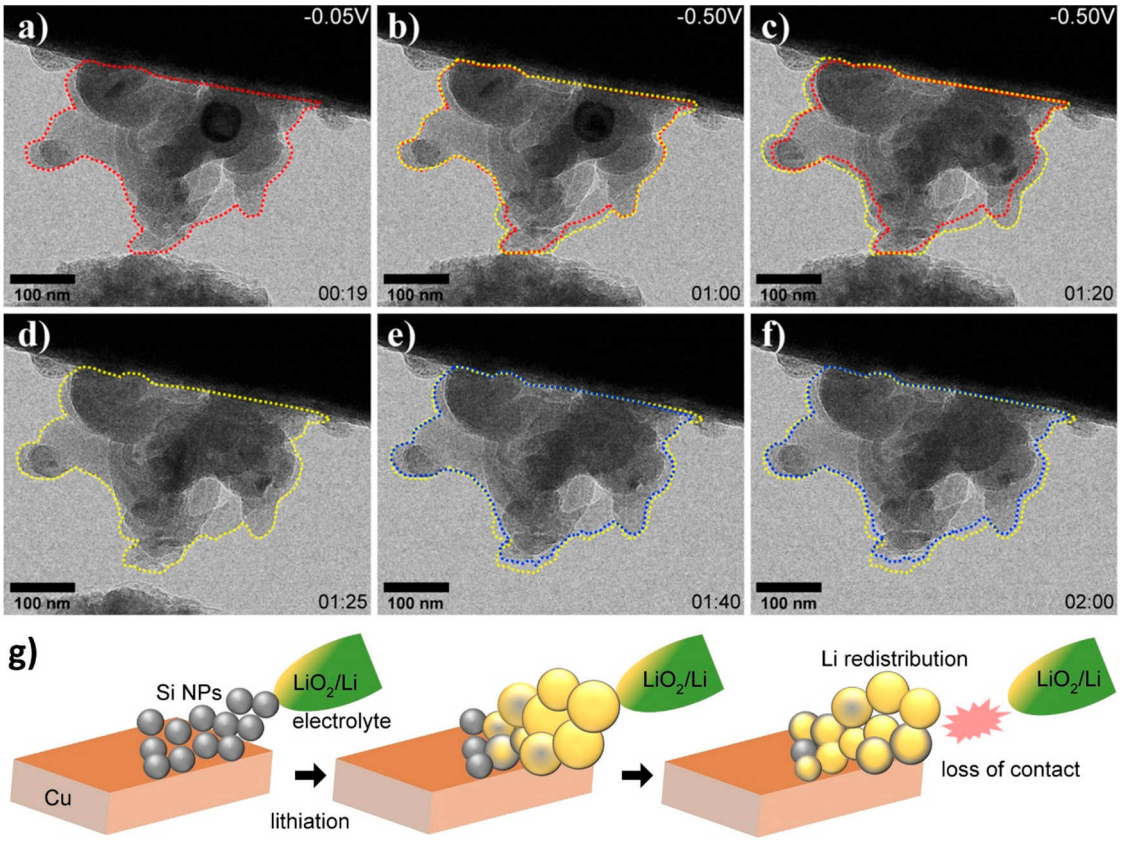

Figure 3. Lithiation of a cluster of Si nanoparticles and loss of electrode−electrolyte contact. The images in panels a−c show the electrochemical lithiation of a cluster of nanoparticles. The red dotted line marks the shape of the cluster before lithiation. The yellow dotted line marks the shape of the cluster at the indicated point in time during lithiation. The images in panels d−f show contraction of the lithiated cluster of nanoparticles after the electrolyte contact was removed. The yellow dotted line marks the shape of the cluster just before the loss of contact. The blue dotted line marks the shape of the cluster at the indicated point in time after loss of contact. (g) Schematic illustration of Li redistribution as lithiated particles contract.

electropolished tungsten (W) needle, whose tip was modified by scratching the surface of Li foils in an Ar glovebox (O_2 < 1 ppm, H_2O < 1 ppm). The assembled holder was then transferred from the glovebox to the TEM with minimal exposure to air. This resulted in the formation of a thin LiO_x layer on lithium metal that is attached to the W needle which acts as a solid electrolyte in our ASSB experiments (Figure 1c). In this way, we have a better handle on mimicking a typical electrode−electrolyte contact breakdown by simply withdrawing the W needle away from Si active particles during or after (de)lithiation. To ensure that the electron beam effect has no significant impact on (de)lithiation processes of the silicon nanoparticle cluster, the electron beam dose rate was limited to 10 e/Å^2 s^{-1} throughout these *in situ* experiments; thus, the information obtained from these experiments can be directly used to understand the behavior of silicon electrodes in a solid-state battery. Details about sample transfer from the glovebox and TEM[26] parameters can be found in the Supporting Information.

Figure 2a−e illustrates the electrochemical lithiation of a Si NP cluster. The images were recorded while applying a negative voltage of −0.2 V to the NPs (at the top of the image) with respect to LiO_x@Li (at the bottom). It can be observed that the solid electrolyte is in minimum contact with the Si NP cluster, and this situation perfectly mimics a typical electrode−electrolyte interface in an ASSB, where practically only a tiny fraction of the electrode particles tends to be in direct contact with electrolytes.

No volume expansion of the NPs was observed, suggesting that no lithiation of the Si NPs had taken place, until the applied voltage reached −0.2 V. Above this voltage, the NPs expanded in volume, and lithiation can be followed, as shown in Movie S1 in the Supporting Information. Two of the NPs, which are not in direct contact with the LiO_x@Li solid electrolyte, have undergone a significant volume expansion compared to ones that were in direct contact with electrolytes. The volume changes of these particles are highlighted in red and blue lines (Figure 2a−e), and their areas measured from TEM micrographs are shown in Figure 2f. The plots show that, initially, the particles expanded rapidly and after 40 s their expansion then was slowed down. The corresponding current recorded during their lithiation at −0.2 V is shown in Supporting Information (Figure S4).

Although this may look surprising, similar lithiation kinetics was reported by McDowell et al. for Si NPs[17] that were directly in contact with electrolytes[18] and that were attached to particles in direct electrolyte contact. In their study, McDowell et al. observed that the lithiation kinetics of Si NPs (compared to amorphous Si) was not diffusion-limited but rather controlled by dynamic reaction front kinetics. Although no fracture or contact loss was noticeable during the lithiation processes observed in Figure 2, it is conceivable that active particles that undergo repeated (de)lithiation processes can inevitably lead to loss of contact between electrode and electrolyte particles in ASSBs, due to both volume changes and decomposition reactions at interfaces leading to microcracks, which is a major

https://dx.doi.org/10.1021/acsaem.0c00543
ACS Appl. Energy Mater. 2020, 3, 5101−5106

challenge for operating ASSBs with high capacity retention. However, our observation where the few particles that are in direct contact with electrolytes still enable lithiation across particles provides a hint that, at least over a length scale of a few hundred nanometers, the lithiation of NPs does not necessarily rely on direct contact with the electrolyte, if the Si NPs are connected to each other. We note that although this may not be strictly valid for intercalation-based electrodes in terms of interparticle ion diffusion (as in alloying-type), it still provides sufficient insights into ASSB prerequisites with regard to lithium accessibility across electrodes in the case of point contact loss.

Figure 3 shows images recorded during a loss of contact between a Si NP cluster and the LiO_x solid electrolyte (see also Movie S2 in the Supporting Information), where the W needle containing solid electrolytes was purposely retracted to simulate the breakdown of a point contact. In comparison with the cluster shown in Figure 2, a higher voltage of ∼−0.5 V was required for lithiation of this particular cluster, most likely due to the presence of a thicker LiO_x layer or poorer electrical contact between the Cu grid and the NPs. The cluster of NPs (Figure 3a) swells as a result of lithiation (Figure 3b,c) upon maintaining contact with LiO_x@Li solid electrolyte. After lithiation (80 s), the W needle with LiO_x@Li was detached from the Si NPs (corresponding to a partial lithiation). This lithiated cluster of Si NPs began to contract almost instantaneously as shown in Figure 3d−f, and the contraction was significant such that the material resembled almost delithiated particles within a few minutes, although no lithium was not extracted from them by using electric potential (Movie S3). This can be explained by considering that the loss of contact between the electrolyte (LiO_x) and the lithiated NP cluster leaves NPs with varied local Li compositions so that they have different chemical potentials. As a result, lithium from the lithium-rich NPs (which are closest to the lithium source) tends to diffuse into lithium-deficient Si NPs within the cluster until an equilibrium chemical potential can be reached. Therefore, the variation in the chemical potential of lithiated NPs appears to be the main driving force for this interparticle Li diffusion, which is different from the observation of Li-ion distribution via electron holography reported by Yamamoto et al.[27] This process is depicted in Figure 3g. Therefore, combining this with the previous observation where particles that were not in direct contact with electrolyte (Figure 2) have undergone significant volume expansion, it can be argued that the inserted lithium is indeed redistributed among Si particles. In doing so, the volume expansion is also effectively countered by a collective buffer action of NPs that were connected to each other, which is supported by the marked size change of Si NPs in the cluster during lithiation and during lithium redistribution (Figure S5). Unfortunately, since most of the NPs are on top of the Cu grid as depicted in Figure 3g, they are outside of the field of view; therefore, the shrinking process across large NPs network was not visible in the TEM, because the drop-casting process used to disperse the NPs onto the Cu half grid resulted in a major fraction of NPs being deposited on Cu grid bars while only a small amount of Si NPs sticks out. This redistribution of lithium that takes place following a loss of contact with electrolytes has implications for capacity retention in ASSBs. In real-world battery operation, if the contact between the electrode and electrolyte particles is lost, lithium from lithiated electrode particles cannot be recovered over subsequent charge−discharge cycles via the same contact point, and if loss of contacts occurs in large numbers across the electrodes, the onset of capacity decay is inevitable. However, our results imply that, once the electrode−electrolyte contact is lost, the redistribution of lithium to nearby electrode particles via interparticle diffusion provides a means to access lithium via other electrode−electrolyte point contacts of nearby electrode particles within the NPs' network. This means that a high ionic conductivity at both the particle and interparticle levels is essential for ASSBs as it can help re-establish percolation pathways for Li-ion and can potentially minimize capacity fading despite the loss of electrode−electrolyte point contacts. However, quantification of the capacity loss solely due to contact losses is highly challenging due to too many factors that simultaneously contribute to capacity loss. For example, electrolyte decomposition can alone cause capacity fade, and in fact, this *in situ* TEM experimental setup requires huge overpotentials to cycle these microbatteries.

To shed more light on the above observations, it is important to consider the fact that the rate of electrochemical (de)-lithiation of an electrode depends on both ionic and electronic conductivity of the electrode network, either of which can be a rate-limiting factor. We therefore compared the speed of electrochemical lithiation with that of chemical lithiation. We note that the rate of chemical lithiation depends only on the ionic conductivity of particles since this does not involve the application of current. In order to study the effect of chemical lithiation, the LiO_x layer was removed from a small part of LiO_x@Li in the high vacuum environment of the TEM, and a fresh lithium metal surface was exposed directly to a NP cluster. The cluster was kept in contact with the lithium surface without applying a voltage. As expected, the cluster started to swell, as shown in Figure S6 in the Supporting Information. It can be observed from Figure 4 that the rates of chemical and

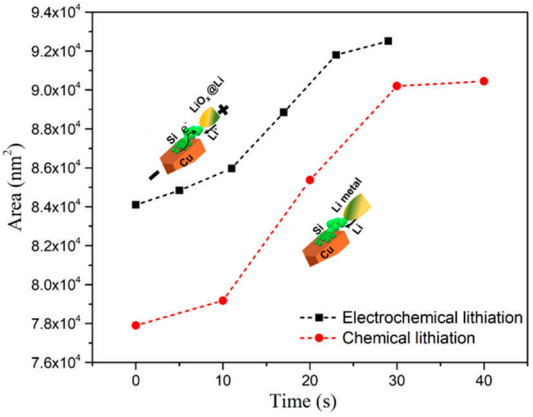

Figure 4. Speeds of chemical and electrochemical lithiation.

electrochemical lithiation are still comparable in terms of the lithium diffusion coefficient in Si (∼5×10^{-12} cm^2/s). However, since the speed of chemical lithiation depends only on ionic conductivity, while the speed of electrochemical lithiation depends on both electronic and ionic conductivity, it can be concluded that electrochemical lithiation of the system in question is not limited by electronic conductivity. In fact, we were also able to electrochemically delithiate the cluster that was chemically lithiated, which looked identical to that of the NP cluster that had undergone electrochemical lithiation and to that of lithium redistribution in terms of their typical volume expansion and contraction as shown in Figure 3 and Movie S2. This therefore establishes that, similar to electrochemical

https://dx.doi.org/10.1021/acsaem.0c00543
ACS Appl. Energy Mater. 2020, 3, 5101−5106

delithiation where Li-ions from lithiated particles are extracted back to electrolytes, upon contact loss the inserted lithium is diffused into other particles and redistributed via interparticle connections, signaled by the particles' relative volume contraction. These changes in the NP cluster during this process can be followed in Movie S3. The corresponding change in cluster area is plotted in Figure S7. Further, the speed of this redistribution that can be approximately estimated from the area change in the field of view was on the order of $\sim 10^{-12}$ cm^2/s, which is comparable to the reported diffusivity of lithium in the crystalline silicon.[28] We emphasize that the lithium redistribution process demonstrated here is limited to mostly Si-based electrode or other alloying-type materials that undergo severe volume change upon (de)lithiation and cannot be generalized to intercalation-type materials such as graphite or other electrode particles (cathodes). It is also important to design cells having multiple electrode−electrolyte interfaces and to perform experiments under a larger field of view to further develop an understanding of the extent to which NPs lithiate without direct electrolyte contact and corresponding lithium redistribution dynamics when electrolyte contacts are broken.

In conclusion, via operando TEM we presented the direct visualization of interface changes in all-solid-state batteries (ASSBs) by utilizing drastically volume changing Si nanoparticles and LiO_x solid electrolyte as a model system during (de)lithiation. From our results, it can be concluded that, at least on a length scale of hundreds of nanometers, lithiation of electrode nanoparticles does not require all electrode particles to be in direct contact with the electrolyte, if electrode particles are interconnected, allowing for Li diffusion via nearby point contacts into the interconnected network of particles. Further, the combination of interparticle connectivity and ionic conductivity of the electrode particles network causes a fast redistribution of lithium between electrode particles upon electrode−electrolyte contact loss. This implies that as the redistributed lithium is still accessible via nearby contact points, this can minimize battery capacity fade over long-term cycling even when few direct electrode−electrolyte contact points are eventually lost. Thus, our study can aid the design of electrodes for high performance ASSBs.

■ ASSOCIATED CONTENT

Supporting Information

The Supporting Information is available free of charge at https://pubs.acs.org/doi/10.1021/acsaem.0c00543.

Methods section and figures and graphs showing (de)lithiation speed (PDF)

Movie S1 showing lithiation of a typical Si NP cluster (AVI)

Movie S2 showing loss of contact between the electrode and electrolyte (AVI)

Movie S3 showing ithiation and delithiation a Si NP cluster during direct contact between Li and Si(AVI)

■ AUTHOR INFORMATION

Corresponding Author

Shibabrata Basak − *Department of Radiation Science and Technology, Delft University of Technology, Delft 2629JB, Netherlands; Institute of Energy and Climate Research, Fundamental Electrochemistry (IEK-9), Forschungszentrum Jülich GmbH, 52425 Jülich, Germany;* orcid.org/0000-0002-4331-4742; Email: s.basak@fz-juelich.de

Authors

Vadim Migunov − *Ernst Ruska-Centre for Microscopy and Spectroscopy with Electrons and Peter Grünberg Institute, Forschungszentrum Jülich GmbH, 52425 Jülich, Germany;* orcid.org/0000-0002-6296-4492

Amir H. Tavabi − *Ernst Ruska-Centre for Microscopy and Spectroscopy with Electrons and Peter Grünberg Institute, Forschungszentrum Jülich GmbH, 52425 Jülich, Germany;* orcid.org/0000-0003-1551-885X

Chandramohan George − *Dyson School of Design Engineering, Imperial College London, SW7 2AZ London, United Kingdom;* orcid.org/0000-0003-2906-6399

Qing Lee − *Department of Radiation Science and Technology, Delft University of Technology, Delft 2629JB, Netherlands*

Paolo Rosi − *Department of Physics, University of Modena and Reggio Emilia, Modena 41125, Italy*

Violetta Arszelewska − *Department of Radiation Science and Technology, Delft University of Technology, Delft 2629JB, Netherlands*

Swapna Ganapathy − *Department of Radiation Science and Technology, Delft University of Technology, Delft 2629JB, Netherlands*

Ashwin Vijay − *Department of Radiation Science and Technology, Delft University of Technology, Delft 2629JB, Netherlands*

Frans Ooms − *Department of Radiation Science and Technology, Delft University of Technology, Delft 2629JB, Netherlands*

Roland Schierholz − *Institute of Energy and Climate Research, Fundamental Electrochemistry (IEK-9), Forschungszentrum Jülich GmbH, 52425 Jülich, Germany*

Hermann Tempel − *Institute of Energy and Climate Research, Fundamental Electrochemistry (IEK-9), Forschungszentrum Jülich GmbH, 52425 Jülich, Germany*

Hans Kungl − *Institute of Energy and Climate Research, Fundamental Electrochemistry (IEK-9), Forschungszentrum Jülich GmbH, 52425 Jülich, Germany*

Joachim Mayer − *Ernst Ruska-Centre for Microscopy and Spectroscopy with Electrons and Peter Grünberg Institute, Forschungszentrum Jülich GmbH, 52425 Jülich, Germany; Central Facility for Electron Microscopy GFE, RWTH Aachen University, 52074 Aachen, Germany*

Rafal E. Dunin-Borkowski − *Ernst Ruska-Centre for Microscopy and Spectroscopy with Electrons and Peter Grünberg Institute, Forschungszentrum Jülich GmbH, 52425 Jülich, Germany*

Rüdiger-A. Eichel − *Institute of Energy and Climate Research, Fundamental Electrochemistry (IEK-9), Forschungszentrum Jülich GmbH, 52425 Jülich, Germany; Institute of Physical Chemistry, RWTH Aachen University, 52074 Aachen, Germany*

Marnix Wagemaker − *Department of Radiation Science and Technology, Delft University of Technology, Delft 2629JB, Netherlands*

Erik M. Kelder − *Department of Radiation Science and Technology, Delft University of Technology, Delft 2629JB, Netherlands*

Complete contact information is available at: https://pubs.acs.org/10.1021/acsaem.0c00543

Notes

The authors declare no competing financial interest.

■ ACKNOWLEDGMENTS

We acknowledge financial support from Shell Global Solutions International BV through a contracted research agreement,

BMBF projects—CatSE (Project 13XP0223A) and LiSi (Project 13XP0224B). We are grateful to Guy Verbist, Wouter Hamer, and Indranil Rudra for fruitful discussions; to Maike Wirtz for help with the glovebox, and to Werner Pieper, Rolf Speen, Michael Farle, and AG Farle at the University of Duisburg-Essen for technical support. V.M. thanks the Deutsche Forschungsgemeinschaft for funding within the framework of the SFB917 Nanoswitches project. C.G. acknowledged FlexBatteries (Grant 704659) from the Marie Skłodowska-Curie action.

REFERENCES

(1) Liu, K.; Liu, Y.; Lin, D.; Pei, A.; Cui, Y. Materials for Lithium-Ion Battery Safety. *Sci. Adv.* **2018**, *4*, eaas9820.
(2) Pham, H. Q.; Lee, H. Y.; Hwang, E. H.; Kwon, Y. G.; Song, S. W. Non-Flammable Organic Liquid Electrolyte for High-Safety and High-Energy Density Li-Ion Batteries. *J. Power Sources* **2018**, *404*, 13.
(3) Henriksen, M.; Vaagsaether, K.; Lundberg, J.; Forseth, S.; Bjerketvedt, D. Explosion Characteristics for Li-Ion Battery Electrolytes at Elevated Temperatures. *J. Hazard. Mater.* **2019**, *371*, 1.
(4) Judez, X.; Eshetu, G. G.; Li, C.; Rodriguez-Martinez, L. M.; Zhang, H.; Armand, M. Opportunities for Rechargeable Solid-State Batteries Based on Li-Intercalation Cathodes. *Joule.* **2018**, *2*, 2208.
(5) Chen, X.; Vereecken, P. M. Solid and Solid-Like Composite Electrolyte for Lithium Ion Batteries: Engineering the Ion Conductivity at Interfaces. *Adv. Mater. Interfaces* **2019**, *6*, 1800899.
(6) Fu, J. Fast Li+ Ion Conducting Glass-Ceramics in the System Li2O-Al2O3-GeO2-P2O 5. *Solid State Ionics* **1997**, *104*, 191.
(7) Murugan, R.; Thangadurai, V.; Weppner, W. Fast Lithium Ion Conduction in Garnet-Type Li7La 3Zr2O12. *Angew. Chem., Int. Ed.* **2007**, *46*, 7778.
(8) Wu, F.; Fitzhugh, W.; Ye, L.; Ning, J.; Li, X. Advanced Sulfide Solid Electrolyte by Core-Shell Structural Design. *Nat. Commun.* **2018**, 4037 DOI: 10.1038/s41467-018-06123-2.
(9) Shoji, M.; Cheng, E. J.; Kimura, T.; Kanamura, K. Recent Progress for All Solid State Battery Using Sulfide and Oxide Solid Electrolytes. *J. Phys. D: Appl. Phys.* **2019**, *52*, 103001.
(10) Hayashi, A.; Sakuda, A.; Tatsumisago, M. Development of Sulfide Solid Electrolytes and Interface Formation Processes for Bulk-Type All-Solid-State Li and Na Batteries. *Front. Energy Res.* **2016**. DOI: 10.3389/fenrg.2016.00025.
(11) Yu, C.; Ganapathy, S.; Van Eck, E. R. H.; Van Eijck, L.; Basak, S.; Liu, Y.; Zhang, L.; Zandbergen, H. W.; Wagemaker, M. Revealing the Relation between the Structure, Li-Ion Conductivity and Solid-State Battery Performance of the Argyrodite Li6PS5Br Solid Electrolyte. *J. Mater. Chem. A* **2017**, *5*, 21178.
(12) Chen, R.; Li, Q.; Yu, X.; Chen, L.; Li, H. Approaching Practically Accessible Solid-State Batteries: Stability Issues Related to Solid Electrolytes and Interfaces. *Chem. Rev.* **2019**. DOI: 10.1021/acs.chemrev.9b00268.
(13) Yu, S.; Mertens, A.; Tempel, H.; Schierholz, R.; Kungl, H.; Eichel, R. A. Monolithic All-Phosphate Solid-State Lithium-Ion Battery with Improved Interfacial Compatibility. *ACS Appl. Mater. Interfaces* **2018**, *10*, 22264.
(14) Takada, K.; Ohno, T.; Ohta, N.; Ohnishi, T.; Tanaka, Y. Positive and Negative Aspects of Interfaces in Solid-State Batteries. *ACS Energy Lett.* **2018**, *3*, 98.
(15) Xu, L.; Tang, S.; Cheng, Y.; Wang, K.; Liang, J.; Liu, C.; Cao, Y. C.; Wei, F.; Mai, L. Interfaces in Solid-State Lithium Batteries. *Joule.* **2018**, *2*, 1991.
(16) Yu, C.; Ganapathy, S.; Eck, E. R. H. V.; Wang, H.; Basak, S.; Li, Z.; Wagemaker, M. Accessing the Bottleneck in All-Solid State Batteries, Lithium-Ion Transport over the Solid-Electrolyte-Electrode Interface. *Nat. Commun.* **2017**, 1086 DOI: 10.1038/s41467-017-01187-y.
(17) Zhao, Y.; Zheng, K.; Sun, X. Addressing Interfacial Issues in Liquid-Based and Solid-State Batteries by Atomic and Molecular Layer Deposition. *Joule.* **2018**, *2*, 2583.
(18) McDowell, M. T.; Ryu, I.; Lee, S. W.; Wang, C.; Nix, W. D.; Cui, Y. Studying the Kinetics of Crystalline Silicon Nanoparticle Lithiation with in Situ Transmission Electron Microscopy. *Adv. Mater.* **2012**, *24*, 6034.
(19) McDowell, M. T.; Lee, S. W.; Harris, J. T.; Korgel, B. A.; Wang, C.; Nix, W. D.; Cui, Y. In Situ TEM of Two-Phase Lithiation of Amorphous Silicon Nanospheres. *Nano Lett.* **2013**, *13*, 758.
(20) Yuk, J. M.; Seo, H. K.; Choi, J. W.; Lee, J. Y. Anisotropic Lithiation Onset in Silicon Nanoparticle Anode Revealed by in Situ Graphene Liquid Cell Electron Microscopy. *ACS Nano* **2014**, *8*, 7478.
(21) Luo, L.; Wu, J.; Luo, J.; Huang, J.; Dravid, V. P. Dynamics of Electrochemical Lithiation/Delithiation of Graphene- Encapsulated Silicon Nanoparticles Studied by in-Situ TEM. *Sci. Rep.* **2015**, 3863 DOI: 10.1038/srep03863.
(22) Dong, L.; Shou, K.; Frutiger, D. R.; Subramanian, A.; Zhang, L.; Nelson, B. J.; Tao, X.; Zhang, X. Engineering Multiwalled Carbon Nanotubes inside a Transmission Electron Microscope Using Nanorobotic Manipulation. *IEEE Trans. Nanotechnol.* **2008**, *7*, 508.
(23) Liu, X. H.; Huang, J. Y. In Situ TEM Electrochemistry of Anode Materials in Lithium Ion Batteries. *Energy Environ. Sci.* **2011**, *4* (10), 3844.
(24) Liu, X. H.; Liu, Y.; Kushima, A.; Zhang, S.; Zhu, T.; Li, J.; Huang, J. Y. In Situ TEM Experiments of Electrochemical Lithiation and Delithiation of Individual Nanostructures. *Adv. Energy Mater.* **2012**, *2*, 722.
(25) Liu, X. H.; Zhong, L.; Huang, S.; Mao, S. X.; Zhu, T.; Huang, J. Y. Size-Dependent Fracture of Silicon Nanoparticles during Lithiation. *ACS Nano* **2012**, *6*, 1522.
(26) Boothroyd, C.; Kovács, A.; Tillmann, K. FEI Titan G2 60—300 HOLO. *J. Large-Scale Res. Facil. JLSRF* **2016**, A44 DOI: 10.17815/jlsrf-2-70.
(27) Yamamoto, K.; Iriyama, Y.; Asaka, T.; Hirayama, T.; Fujita, H.; Fisher, C. A. J.; Nonaka, K.; Sugita, Y.; Ogumi, Z. Dynamic Visualization of the Electric Potential in an All-Solid-State Rechargeable Lithium Battery. *Angew. Chem., Int. Ed.* **2010**, *49*, 4414.
(28) He, Y.; Piper, D. M.; Gu, M.; Travis, J. J.; George, S. M.; Lee, S. H.; Genc, A.; Pullan, L.; Liu, J.; Mao, S. X. In Situ Transmission Electron Microscopy Probing of Native Oxide and Artificial Layers on Silicon Nanoparticles for Lithium Ion Batteries. *ACS Nano* **2014**, *8*, 11816.

https://dx.doi.org/10.1021/acsaem.0c00543
ACS Appl. Energy Mater. 2020, 3, 5101—5106